

An Experimental Investigation into the Execution of Microchannel Heat Sinks in Forced Convection Heat Transfer

Maniratan Singh¹, Hemant Kumar², Harry Garg³

¹ Department of Mechanical Engineering, Punjabi University, Patiala – 147002, India.

² Department of Mechanical Engineering, Punjabi University, Patiala - 147002, India.

³ CSIR-Central Scientific Instruments Organisation, Chandigarh - 160030, India.

Abstract

Heat transfer in microelectronics provides a wide range of theoretical, analytical and experimental challenges. In the present numerical and experimental study, forced convection heat transfer in microchannel heat sinks was observed tentatively. During study two different configurations of microchannels; Upstream Triangular microchannel and downstream triangular microchannel are compared with the rectangular microchannel. Geometrical parameters of microchannel were varied i.e. channel length was likewise changed from 15 - 22mm, channel width was varied from 0.5 - 1mm and fin height was varied from 2 - 7mm to get the optimum shape of a microchannel with maximum heat transfer coefficient. 14 microchannels are fabricated on copper plate. It is found that heat transfer in downstream microchannel is better than upstream and rectangular microchannel at very low Reynolds number. The Nusselt number measured increased with increasing Reynolds number during laminar flow regime. It was also reported that Reynolds number was ranging from 7 to 450 in proposed shapes of microchannel considering laminar flow. DI water was used as working fluid in microchannel heat sinks. It is investigated that average heat transfer enhancement by using optimum geometry is 3-4 times with acceptable friction loss.

Keywords: Microchannel; nanofluid; CFD; heat sink; electronic cooling

INTRODUCTION

Heat expulsion in an effective way is vital, keeping in mind the end goal to keep up the solid operations of electronic devices. The size of electronic devices diminishes ordinary because of the packing of a vast number of circuits in a given space. So as to enhance the speed of devices, the circuit power must be enhanced, which prompts a heat generation. This has made the cooling system huger, and thermal management of electronic contraptions has turned into an essential issue. The solutions for such systems ought to be examined precisely. Such arrangements comprise heat transfer by conduction, heat transfer by convection and radiation heat transfer. Be that as it may, these methods of heat transfer are entwined, in this manner, heat transfer issues get all the more difficult. Forced convection is generally utilized a technique for cooling, and liquid(water) cooling is a standout amongst the most custom strategies (Phillips, 1987). Also, the design of forced convection liquid cooling system is simple and economic; the system has high quality and simple maintenance (Mehendale

et al., 2009). The most well-known methods for improving forced convection liquid cooling system are utilizing microchannel heat sinks (Kandlikar, 2005). The heat transfer rate of a surface can be enhanced by enhancing heat transfer coefficient, h and by enhancing the surface area, A , if the power input and temperature points of confinement are altered according to Newton's law of cooling, $Q=h.A.\Delta T$. Since the heat transfer coefficient cannot be controlled autonomously, so we ought to need to increase and optimize the surface area to get an upgrade in heat transfer. Fins are the least demanding approach to expand the surface area.

As fins expand, the surface area additionally builds the imperviousness to the stream of working fluid. The heat transfer coefficient in view of the base area of fin array exhibit might be not as much as that of the base plate. Due to this reason, the reduction in the heat transfer coefficient is more than the expansion in the surface area, consequently the aggregate heat transfer rate decrease (Yadav et al., 2016). In this way, the size and shape of microchannel heat sinks ought to be optimized. Comprehensive literature has demonstrated that different theoretical and experimental works have been performed on different microchannel heat sinks (Akbar et al., 2014). A few numerical and experimental have been done on vertical plates (Yang et al., 2014). Different channels configurations have additionally been researched, however, the utilization of such designs is restricted (Xia et al., 2015). The most well-known arrangements include flat and vertical surfaces to which plate or pin fin arrays attached. Such arrangements have been examined by numerous authors to decide their heat transfer exhibitions (Yifan et al. 2017).

In the present study, a more extensive range of parameters are explored to decide the convection heat transfer execution of differently designed microchannel heat sinks. The fundamental targets of the study are; to direct point by point and careful examinations on different microchannel heat sinks, to decide the impacts of geometric parameters, channel length and channel width, channel length and velocity of working fluid on the heat transfer execution of microchannel heat sinks, to locate the ideal parameters that will augment the heat transfer execution of microchannel heat sinks.

DEVICE DESIGN AND FABRICATION

Design of microchannels was done on Solid works 2014. Proposed microchannels shapes when used with water as a coolant showed high heat transfer rate. Furthermore, poor conductivity issue could be overcome with the use of high

convection rate of microchannels. The geometrical aspects of microchannels are the width of the microchannel, the height of microchannel, length of microchannel. Rectangular, Upstream and downstream microchannel 3D geometry are shown in Figure 1 and geometric and characteristic parameters are outlined in Table 1. The substrate was made up of copper material because of high thermal conductivity 385W/mK and channels were further fabricated by using micro precision wire EDM machine on a substrate made up of copper.

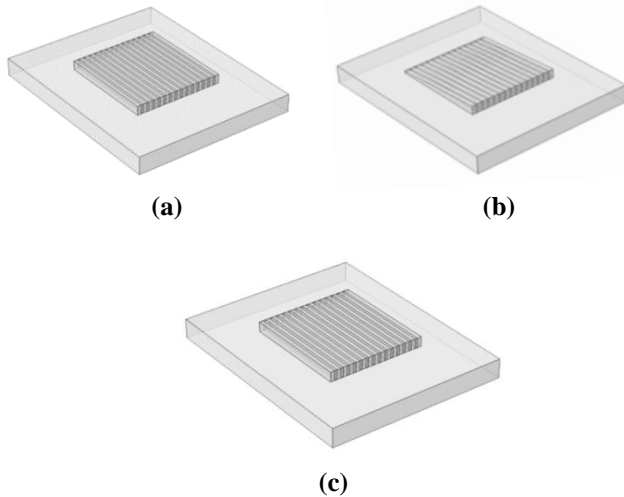


Figure 1 (a) Downstream triangular (b) rectangular (c) upstream triangular

EXPERIMENTAL EQUIPMENT AND INSTRUMENTATION

The setup principally comprises of a silicon sheet pad for supporting microchannel heat sink and calculate the ambient temperature, base plate temperature, and input power for the heater various instruments were used. A schematic perspective of experimental setup is shown in Figure 2. The microchannel heat sink was designed predominantly taking into account the manufacture of conceivable outcomes accessible. The heat sink was intended to be made out of parallel microchannel with rectangular cross sections, for a simple layout. The test module shown in Figure 3 was fabricated from a copper substrate and used a polycarbonate cover, which served as both insulator and sealant. 14 rectangular cross-sectional microchannel designs, 22 mm long each, were fabricated and evaluated. The Geometric and Characteristic parameters of channel are given in Table 1.

Table 1. Geometric and characteristic parameters

S. No.	Microchannel	Height (mm)	Length (mm)	Width (mm)	Mass Flow Rate (ml/min)
1.	Rectangular	2-7	15-22	0.5-0.8	5-25
2.	Upstream triangular	2-7	15-22	0.5-0.8	5-25
3.	Downstream triangular	2-7	15-22	0.5-0.8	5-25

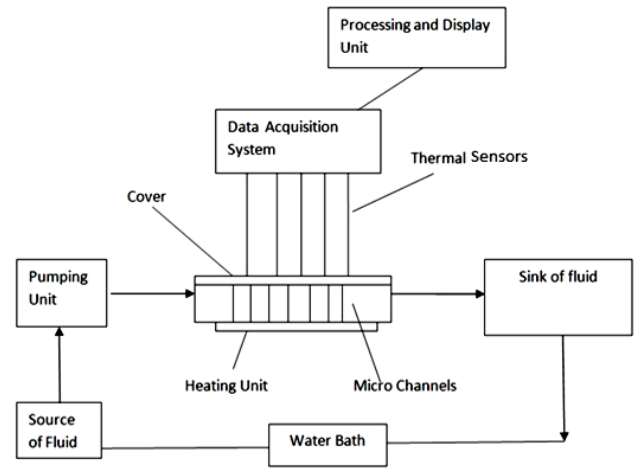


Figure 2. Schematic view of experimental setup

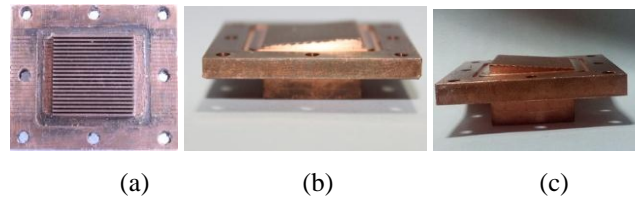


Figure 3. Fabricated model of (a) rectangular microchannel (b) upstream triangular microchannel (c) downstream triangular microchannel

Two plenums were machined on polycarbonate cover plate and associated with the microchannel to frame the test section. Two thermocouples were likewise introduced in the entrance and exit plenums, to measure the fluid temperature. Moreover, one thermocouple was introduced on the back of the test section to measure the wall temperature of the microchannel. During the experiment, the test article was put in an insulated lodging to minimize the heat misfortune because of convection and radiation. Experiments were conducted at inlet fluid temperatures ranging from 15°C to 22°C, relating to a fluid subcooling range of roughly 38-82°C. Fluid Mass flow rate went from 5 to 30 ml/min. In the majority of the tests, the flow rate of the working fluid entering the test article was measured utilizing a peristaltic pump, and its extent was controlled via automatically adjustable pumping power. The inlet fluid temperature was kept up at a consistent quality utilizing the heat exchanger set as a part of the test loop by heating or cooling.

The copper substrate was electrically heated by direct interfacing the test section to a plate heater which further connected with a transformer that provided low voltage and high electric current. In this way, heat produced in the substrate or plate was exchanged to the fluid flow from the two sides and base of the microchannel. As a result of the Joule heating, the heat flux was assumed to be uniform and consistent along the longitudinal length and the wetted periphery, with the exception of the top surface, which was insulated as shown in Figure 4. The input voltage and current could be changed in accordance with the control of the input

power and were utilized to decide the connected heat flux. Experiments were conducted under steady state conditions. For each design, the fluid flow rate, fluid temperatures, inlet and outlet pressure, wall surface temperatures, input voltage, and currents were all deliberate and recorded.

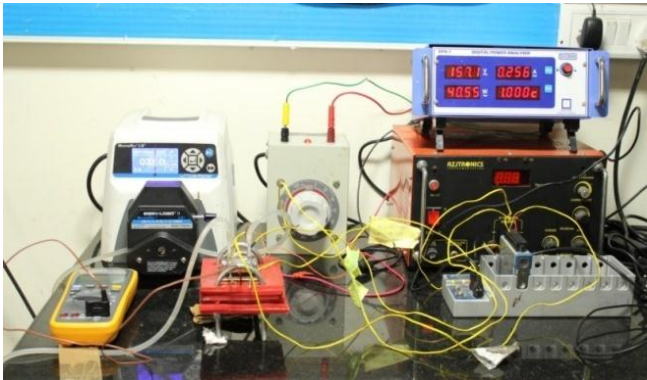


Figure 4. Microchannel experimental setup

NUMERICAL AND EXPERIMENTAL ANALYSIS

The geometries were modeled to carry out the numerical analysis. Exactness in the numerical computations was upgraded by assuming all boundary conditions, constraints, inlet and outlet positions. In the present study, three different setups were assessed from coarse to finer networks. Increase in a number of elements is a trade-off past the confinements of computational time. The COMSOL Multiphysics software was used for numerical computations. To further validate the numerical model, the predicted temperature was compared with the measurement of the practical setup at a full scale. The predictions are generally within 1°C of the measured results.

Assumptions

1. Input heat flux to the base of the microchannel is assumed to be constant and steady.
1. Hence, utilization of consistent heat flux is assumed for simulation.
2. Flow regime is laminar, incompressible, single phase and steady.
3. There is no heat transfer from the top and region around inlet and outlet.
4. Constant fluid properties.
5. Negligible convective as well as radiation heat transfer to the surroundings which further assumed zero.

Governing equations

Continuity equations

$$\nabla \cdot (\rho u) = 0 \quad (1)$$

Momentum equations

$$\rho(u \cdot \nabla)u = \nabla \cdot \left[-pI + \mu \left(\nabla u + (\nabla u)^T - \frac{2}{3} \mu (\nabla \cdot u) I \right) + F \right] \quad (2)$$

Energy equations fluid

$$\rho C_p u \cdot \nabla T = \nabla \cdot (k \nabla T) + Q + Q_{vh} + W_p \quad (3)$$

Solid

$$\rho C_p u \cdot \nabla T = \nabla \cdot (K \nabla T) + Q \quad (4)$$

Initial value

$$u = 0, P = 0, T = 293.15K$$

Fluid walls:

Boundary condition

No Slip, $u = 0$

Inlet: -

$$u = -u_0 n = \text{normal inflow velocity}$$

$$T = T_0 = 295.15K = \text{inlet temperature}$$

Outlet:

Boundary conditions, pressure, viscous stress

$$P = P_0 = 0, \left[\mu \left(\nabla u + (\nabla u)^T - \frac{2}{3} \mu (\nabla \cdot u) I \right) \right] n = 0 \quad (5)$$

Outflow

$$-n \cdot (-K \nabla T) = 0$$

Heat flux

$$n \cdot (-K \nabla T) = \frac{Q_{tot}}{A}, Q_{tot} = \text{input} \quad (6)$$

power 100W

The analysis was carried out using different Reynolds number for working fluid.

$$Re = \frac{\rho V_{avg} D}{\mu} = \frac{V_{avg}}{\nu} \quad (7)$$

where V_{avg} is the average flow velocity, D is the diameter of the tube, and ν is the kinematic viscosity of the fluid. For flow through noncircular tubes, the Reynolds number as well as the Nusselt number and the friction factor are based on the hydraulic diameter D_h instead of D defined as

$$D_h = \frac{4A_c}{p} \quad (8)$$

Friction Factor

$$f = \frac{2d_h \Delta P}{\rho u^2 L} \quad (9)$$

$$Nu = \frac{h D_h}{K} = \frac{D_h}{K} \left(\frac{m c_p (T_{ot} - T_i)}{A (T_s - T_m)} \right) \quad (10)$$

GRID INDEPENDENCE TEST

Grid independence study has been completed before examination keeping in mind the inaccuracy developed because of coarseness of grids. Table 2 demonstrates the summary of three grid system for all the purposed designs. Complete computational domain has been discredited utilizing an unstructured grid of tetrahedral volume elements. Finer meshing has been received for the finned surface and for the water fluid domain regions, as parameters like temperature, weight, and speed are more sensitive in these regions. The outcomes got for various grid systems have been thought about and it is watched that the arrangements by the last two grid system for all cases are near each other, outlet temperature and weight drop varieties are under 0.2%. Subsequently, keeping in mind the end goal to spare calculation time intermediate grid system 2 has been utilized for both designs as a part of final CFD investigation.

Table 2. Summary of grid independence study

Grid system	Number of elements		
	Rectangular	Upstream triangular	Downstream triangular
1	77060	62283	62283
2	36840	30621	30621
3	25304	20196	20196

RESULTS AND DISCUSSIONS

Physical parameters like temperature, heat transfer coefficient and friction factor are considered here for the determination of heat transfer in the microchannel. Apart from these, different geometries are proposed for different aspect ratio at different velocities at the inlet of the microchannel. Finally, the comparison between experimental and numerical results has been done.

Temperature variations

Due to change in the geometry of microchannel heat sinks temperature variation occurs. Here, a variation of temperature in various geometries of the microchannel heat sinks was obtained. Temperature distribution could be closely observed in Figure 5 for rectangular, upstream triangular and downstream triangular microchannel heat sinks. These contours are obtained for inlet velocity of 0.0005m/s. It was found that temperature surrounding the inlet region is low and increasing along the length from inlet to outlet. This is because of the development of thermal boundary layer that heat transfer in beginning is large and decreases along the direction of flow. Comparing temperature distribution contours among the three different geometries, the thermal boundary layer gets developed soon along the length for downstream triangular geometry than rectangular geometry, and because of this reason downstream triangular geometry have greater heat transfer coefficient as compared to other two geometries, and this can also be observed in Figure 5(a), (b), (c) respectively.

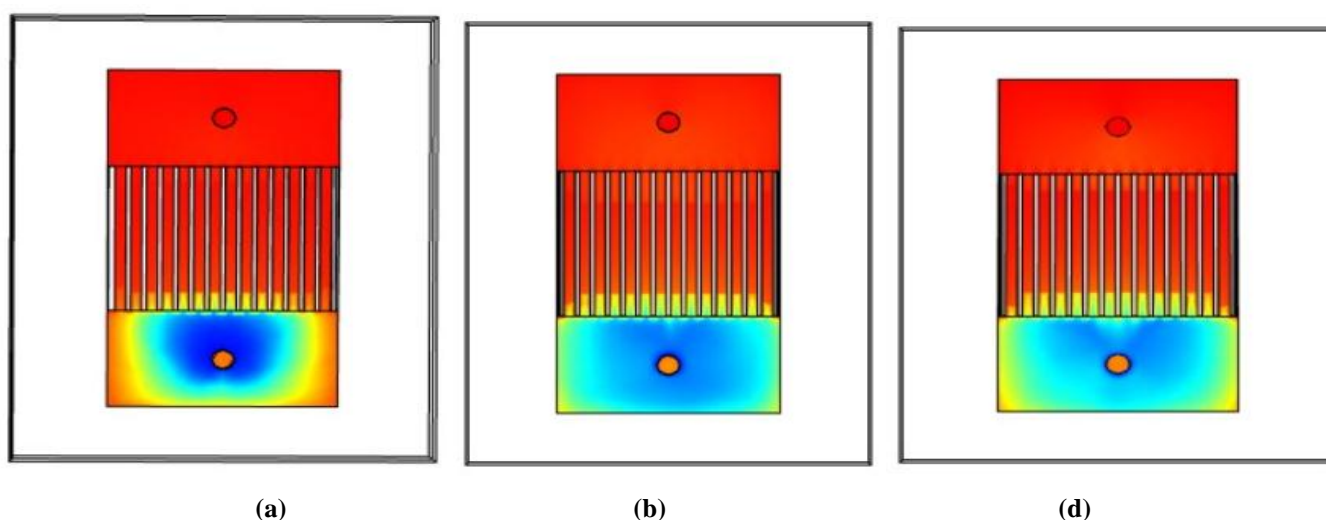


Figure 5. Temperature contour for (a) rectangular (b) upstream triangular (c) downstream triangular

Comparison among different geometries at different fluid velocities

Here, heat transfer is analyzed for rectangular geometry. Cooling effect increases with increase in inlet velocity of fluid, as shown in Figure 6. Heat transfer effect is much high in the case of downstream triangular geometry when compared with upstream triangular and rectangular geometry. At a maximum velocity of 0.00042m/s the heat transfer coefficient is 5.04, 6.12 and 9.2 kW/m²K for rectangular, upstream triangular and downstream triangular microchannel heat sinks respectively.

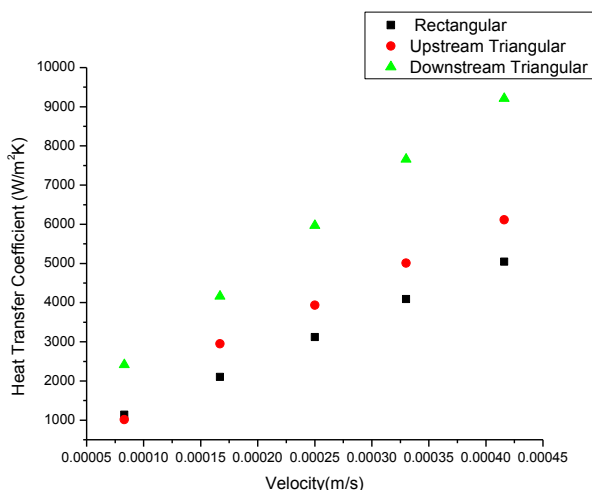


Figure 6. Heat transfer coefficient variation with fluid velocity

Comparison among different geometries at different channel length

Channel length is analyzed for various geometries. There is different effect of channel length on different geometries in rectangular geometry. The channel length ranges from 15mm to 22mm. Cooling effect first decreases then increases gradually with increase in channel length. In upstream triangular geometry, cooling effect increases as channel length increases and in downstream triangular geometry, cooling effect decreases as channel length increases as shown in Figure 7. At maximum channel height 22mm the heat transfer coefficient is 5.04, 5.99 and 9.2 kW/m²K for rectangular, upstream triangular and downstream triangular microchannel heat sinks respectively.

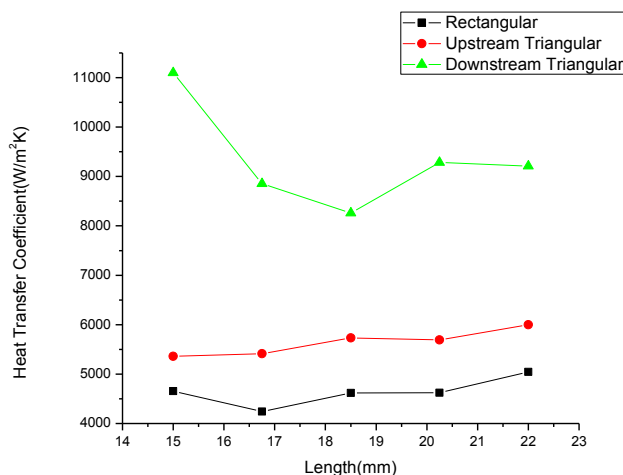


Figure 7. Heat transfer variation along length

Comparison among different geometries at different channel width

Figure 8 displays the effect of channel width over heat transfer coefficient of microchannel heat sinks. The width of channel ranges from 0.5mm to 1mm. As the channel width increases the cooling effect of microchannel heat sinks first decrease slightly then increases rapidly. At maximum channel width of 1mm, the heat transfer coefficient obtained is 10.08, 12.31 and 14.99 kW/m²K for rectangular, upstream triangular and downstream triangular microchannel heat sinks respectively.

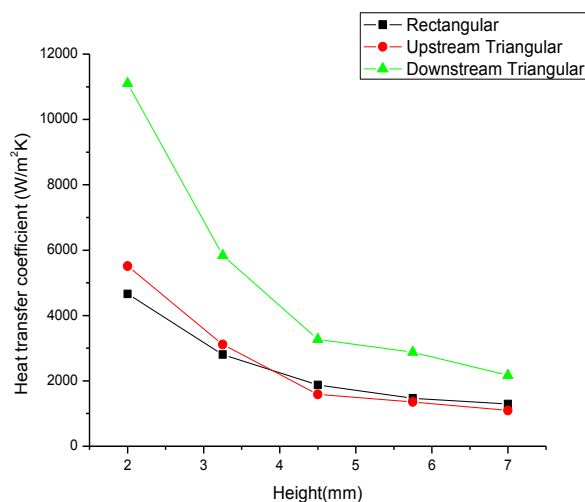


Figure 8. Heat transfer variation with width

Comparison of different geometries at different channel height

In Figure 9, convective heat transfer coefficient is plot a function of channel height to see its effect clearly. The channel height ranges from 2mm to 7mm. it can be observed

that as channel height increases the heat transfer coefficient decreases. At channel height of 2mm, the heat transfer coefficient obtained is 4.65, 5.51 and 11.1 kW/m²K for rectangular, upstream triangular and downstream triangular microchannel heat sinks respectively.

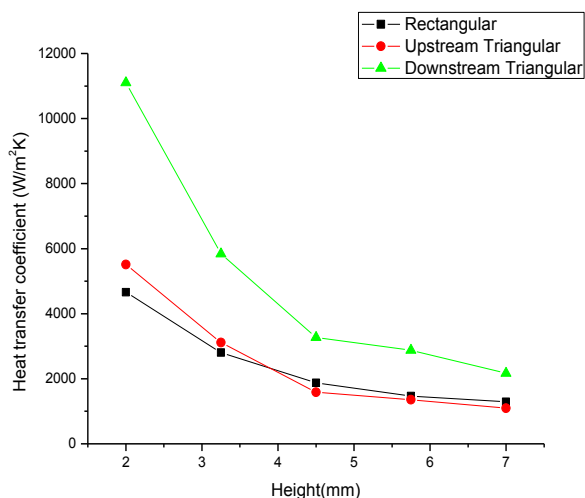


Figure 9. Heat transfer variation with height

Comparison of experimental results and numerical simulation

The experimental results are tabulated in Table 3 using all parameters and different microchannel heat sink geometries at same heat flux. Better heat transfer enhancement is achieved as the optimal parameters are used for the fabrication and experimentation. For various geometries the heat transfer ratio is greater than 1 as compared to rectangular geometry for which it may be high as 4. This reveals that good enhancement is attached by using optimum parameters and rectangular geometry. Heat transfer increases with increase in inlet velocity in general for all given geometries but, here also heat transfer for downstream triangular geometry is much greater in magnitude than upstream triangular and rectangular microchannel heat sink as shown in Figure 10.

Table 3. Experimental versus numerical values

Velocity (m/sec)	Numerical value of h (W/m ² K)	Experimental value of h (W/m ² K)
0.00083	6221	5054
0.00167	9239.5	8621
0.00250	11935	10875
0.00333	13774	11995
0.00416	14996	14005
0.005	15688	13887

The heat transfer coefficient varies uniformly for upstream triangular and rectangular microchannel heat sinks. But in case of downstream triangular microchannel heat sink, there is a large variation from inlet plenum to outlet plenum. The

average thermal gradient across the interfaces microchannel wall and fluid is very less as compared to upstream triangular and rectangular heat microchannel sink. Heat transfer coefficient increases with an increase in the magnitude of flow velocity. Up to inlet velocity 0.0005 m/s fluid resides in laminar regime (R_e less than 1000). With further increase in inlet velocity, Reynolds number exceeds due to which laminar flow becomes turbulent. Hence, higher velocities are not considered for the present study.

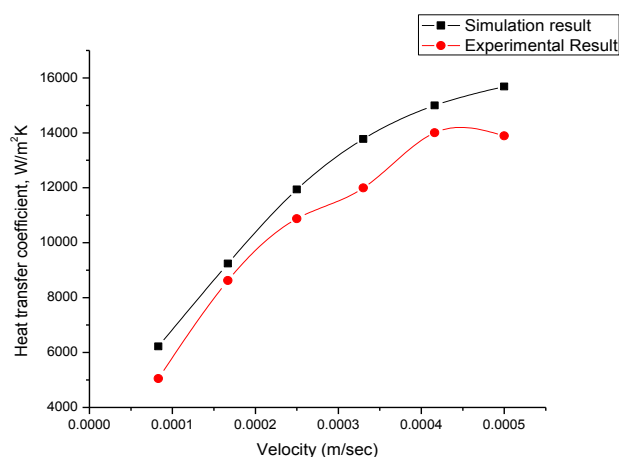


Figure 10. Velocity versus heat transfer coefficient

CONCLUSION

The results of experiments were presented so as to delineate the effect of geometry as well as various parameters on the performance of microchannel heat sinks. Several conclusions may be deduced from this study.

The heat transfer coefficient for any microchannel heat sink depends strongly on geometry of microchannel heat sink and on various parameters used. For a given velocity of working fluid, heat transfer coefficient increases as we move from rectangular, upstream triangular then downstream triangular geometry. At a given channel length, the heat transfer coefficient has a little increment in upstream triangular geometry when compared with rectangular geometry, but there is a great increase in downstream triangular geometry. Channel width also has a great effect on heat transfer coefficient of all geometries. As the channel width increases, the total surface area of channel increase, thus the heat transfer coefficient increases. However, the closer channels cause resistance to flow, the boundary layers start to interfere and after a certain value further increase in the area starts to decrease the heat transfer coefficient. Therefore, for the maximum heat transfer rate, the channel width should be kept at an optimum value.

Similarly, the channel length and channel height has a great influence on performance of microchannel heat sink. As the channel length increases, the heat transfer coefficient slightly increases for rectangular and upstream triangular geometry, but in downstream triangular geometry, heat transfer

coefficient get decreases with respect to channel length. So here we can have concluded that the geometry also has an influence as well as geometry parameters of microchannel heat sinks.

As channel height increases, the heat transfer coefficient decreases rapidly, so smaller but optimum height is recommended to use for maximum heat transfer coefficient of microchannel heat sinks. A comparison of various geometries with different parameters shows that, the downstream triangular geometry of microchannel heat sinks has great performance as compared to other geometries.

NOMENCLATURE

K (W/mK)	Thermal conductivity	Q_{tot} (W)	Input power
Re	Reynolds number	Q (W)	Heat input to the microchannel
Nu	Nusselt number	T_i (K)	Temperature at the inlet
h (W/m ² K)	Heat transfer coefficient	T_0 (K)	Reference temperature
u (m/sec)	Fluid velocity	V (m/s)	Magnitude of average velocity
m (kg/sec)	Mass flow rate	ρ (kg/m ³)	Density

REFERENCES

- [1] Akbar, N.S., Raza, M. and Ellahi, R. (2014) 'Interaction of nanoparticles for the peristaltic flow in an asymmetric channel with the induced magnetic field', *The European Physical Journal Plus*, doi 10.1140/epjp/i2014-14155-6.
- [2] Kandlikar, S.G. (2005) 'High heat flux removal with microchannels – A roadmap of challenges and opportunities', *Heat Transfer Engineering*, Vol. 26, No. 8, pp. 5-14.
- [3] Mehendale, S. S., Jacobi, A. M., and Shah, R. K. (2009) 'Fluid flow and heat transfer at micro- and meso-scales with applications to heat exchanger design', *Applied Mechanics. Reviews*, Vol. 53, pp. 175–193.
- [4] Phillips, R. J. (1987) 'Forced convection, liquid cooled, microchannel heat sinks', MS Thesis, Department of Mechanical Engineering, Massachusetts Institute of Technology, Cambridge, MA.
- [5] Xia, G.D., Jiang, J., Wang, J., Zhai, Y.L. and Ma, D.D. (2015) 'Effects of different geometric structures on fluid flow and heat transfer performance in microchannel heat sinks', *International Journal of Heat and Mass Transfer*, Vol. 80, pp. 439–447.
- [6] Yadav, V., Baghel, K., Kumar, R. and Kadam, S.T. (2016) Numerical investigation of heat transfer in extended surface Microchannels', *International Journal of Heat and Mass Transfer*, vol. 93, pp. 612–622.
- [7] Yang, L., Dua, K., Niu, X., Zhang, Y. and Li, Y. (2014) 'Numerical investigation of ammonia falling film absorption outside vertical tube with nanofluids', *International Journal of Heat and Mass Transfer*, Vol. 79, pp. 241–250.
- [8] Yifan, L., Guodong, X., Yuting, J., Dandan, M., Cai, B. and Wang, J. (2017) 'Effect of geometric configuration on the laminar flow and heat transfer in microchannel heat sinks with cavities and fins', *Numerical Heat Transfer, Part A: Applications*, Vol. 71, No. 5, pp. 528–546.